FINAL REPORT

Project Title: Frequency Dependent Properties of Magnetic Nanoparticle Crystals
(3/15/12 – 3/14/16)
Institution: Carnegie Mellon University, 5000 Forbes Ave., Pittsburgh, PA 15213
Principal Investigator: Prof. Sara A. Majetich, Physics Dept., 412-268-3105, sara@cmu.edu
DOE/Office of Science Program Office: Materials Sciences and Engineering
DOE/Office of Science Technical Contact: Dr. Refik Kortan
DOE Award Number: DE-FG02-08ER46481

I. OVERVIEW

This research program had three main components related to the properties of magnetic nanoparticles and their interactions: 1) frequency-dependent properties of magnetic nanoparticle assemblies, 2) electron microscopy investigation of magnetic nanoparticles, and 3) polarized neutron scattering of magnetic nanoparticle assemblies. The original objective was to understand the frequency-dependent behavior of magnetic composites made from monodomain nanoparticles with uniform sizes. This was accomplished through studies on nanoparticle assemblies and also magnetization dynamics of single particles. However, careful neutron scattering and electron microscopy experiments showed that the particles themselves were more complex, particularly those made of magnetic oxides. Particles predicted to be single domain based on their size can actually have domain walls if they contain antiphase boundary structural defects [Nedelkowski 2015]. Single crystal particles without defects showed even more surprising behavior when probed by polarized small angle neutron scattering. In remanence the magnetization of the particle is uniform, as expected for single domains, but in large magnetic fields the surface spins cant relative to the interior. The shell thickness could be controlled reversibly through changes in the temperature and magnetic field [Krycka 2015a].

There were 9 papers and one Ph.D. thesis acknowledging support from this grant [Booth 2012], [Krycka 2012, 2015 a,b], [Chowdary 2013, 2014], [Sahkarov 2014], [Stamps 2014], [Hasz 2014], [Nedelkowski 2015].

II. Frequency-Dependent Magnetic Properties of Co, Ni, and FeCo Nanoparticle Composites

The frequency and temperature dependent hysteresis loops (Figure 1) and magnetic permeability (Figure 2) of a $Fe_{10}Co_{90}$ nanoparticle compact were measured over a range of temperatures (77 K - 873 K) and frequencies (0.1 kHz - 100 kHz). The low frequency permeability was roughly independent of temperature, but at higher frequencies the real part rolled off near the maximum in the imaginary part at a characteristic frequency. When normalized to the characteristic frequency and static permeability, the results for different temperatures showed universal scaling. The asymmetry in the Cole-Cole plot was consistent with a distribution of relaxation times. The experimental data were fit by a

modified Cole-Davidson model with extra damping that agreed quantitatively with the predictions due to extra phase lag from eddy current losses [Chowdary 2013, 2014]. At the temperature increases, the distribution of relaxation times narrowed and shifted to shorter values. The characteristic frequency increased roughly exponentially with temperature. This could arise from reduced anisotropy, but likely arises from changes in the skin depth due to the temperature dependence of the electrical resistivity. The analytic approach developed to analyze the $Fe_{10}Co_{90}$ nanocomposite is applicable to other soft magnetic nanocomposites. We developed a toroidal cell and measured the 10 MHz – 10 GHz frequency permeability in Co and Ni particle assemblies [Sakharov 2014].

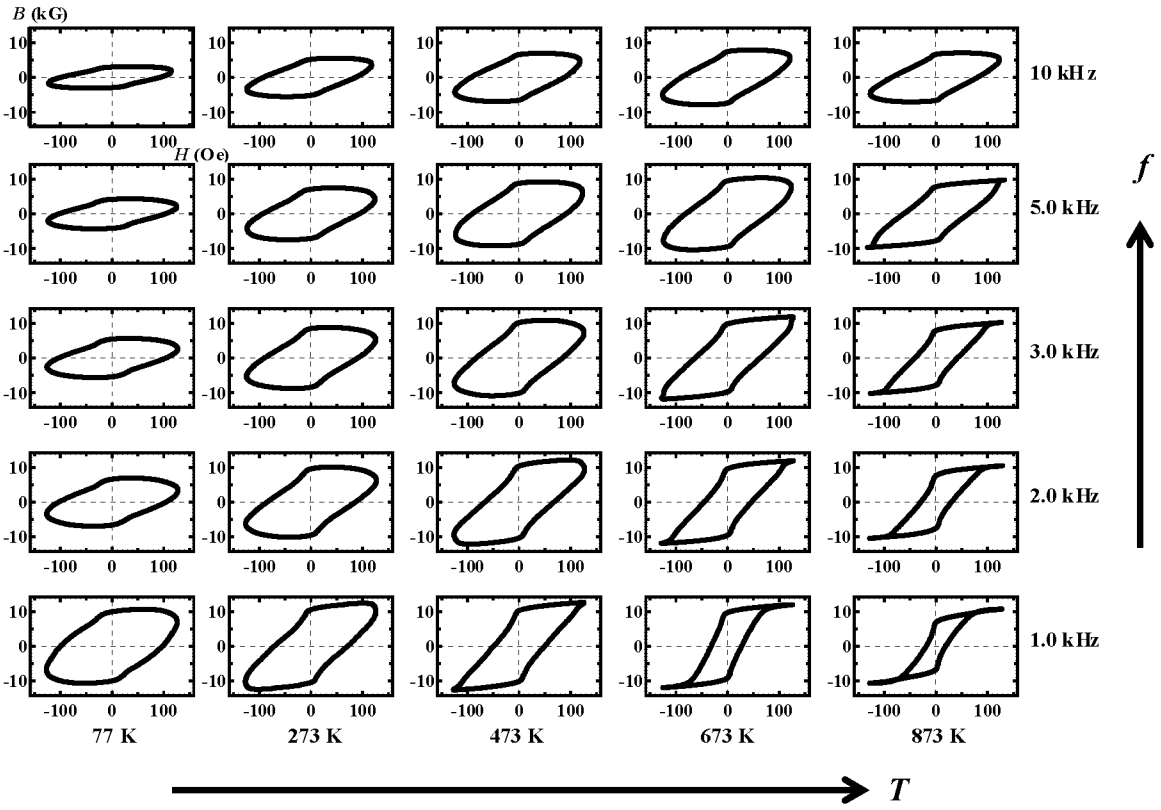

Fig. 1. Selected minor induction hysteresis loops arranged by temperature (horizontal) and frequency (vertical) for temperatures between 77 K and 873 K and moderate frequencies between 1.0 kHz and 10 kHz [Chowdary 2014].

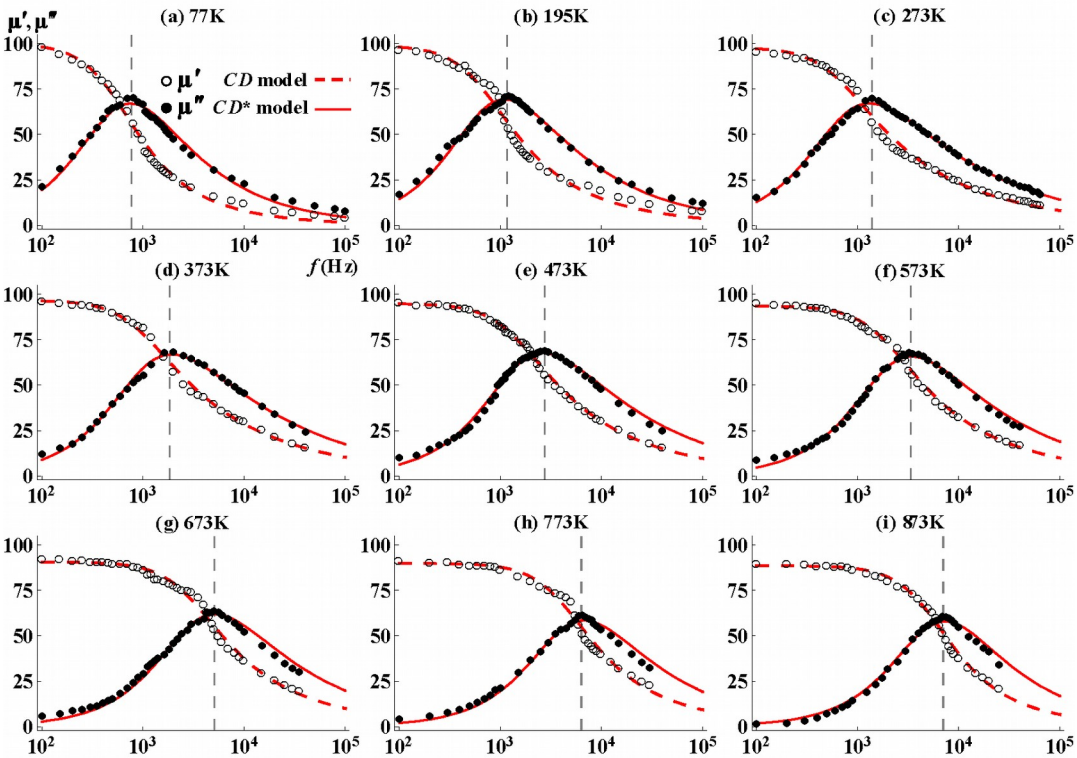

Fig. 2. Modified Cole-Davidson model predictions compared to data. The vertical dashed line indicates f_c. (a) 77 K, (b) 195 K, (c) 273 K, (d) 373 K, (e) 473 K, (f) 573 K, (g) 673 K, (h) 773 K, (i) 873 K [Chowdary 2014].

These data confirmed that magnetic nanoparticle assemblies act as soft ferromagnets, as predicted, and demonstrated that high permeability could be achieved provided the assemblies were dense and formed from high magnetization materials, such as FeCo. However, the thin barriers needed for high magnetization also led to the onset of some eddy current losses at high frequencies. Further work with thicker barriers between particles [Sakharov 2014] greatly reduced the permeability. A thin but more insulating barrier would be needed to push the usable frequency range above 1 MHz.

Magnetic switching frequencies were also measured for single particles using conductive AFM. Here magnetic nanoparticles are deposited on a magnetic thin film and a conductive probe is placed in contact with the top of the particle, and tunnel magnetoresistance is measured. There are characteristic resistance levels depending on the relative angle between the magnetization of the particle and film. Because the crystallographic orientation of a spherical nanoparticle is difficult to control [Piotrowski 2014], cube-shaped Fe_3O_4 nanoparticles were used (Figure 3). In these nanocubes there is competition between magnetocrystalline anisotropy, which would favor magnetization along a body diagonal, and shape anisotropy, which favors magnetization perpendicular to a (100) face. At H = 0, four distinct levels are observed. The magnitudes of the magnetoresistance suggest that shape anisotropy is dominating (maximum current when parallel to the FePt moment, minimum when antiparallel, and ~8.2 μA when directed

perpendicular to the side faces). However, the fourth state at ~8.6 μA may occur when the moment points along one of the body diagonals. This work is ongoing.

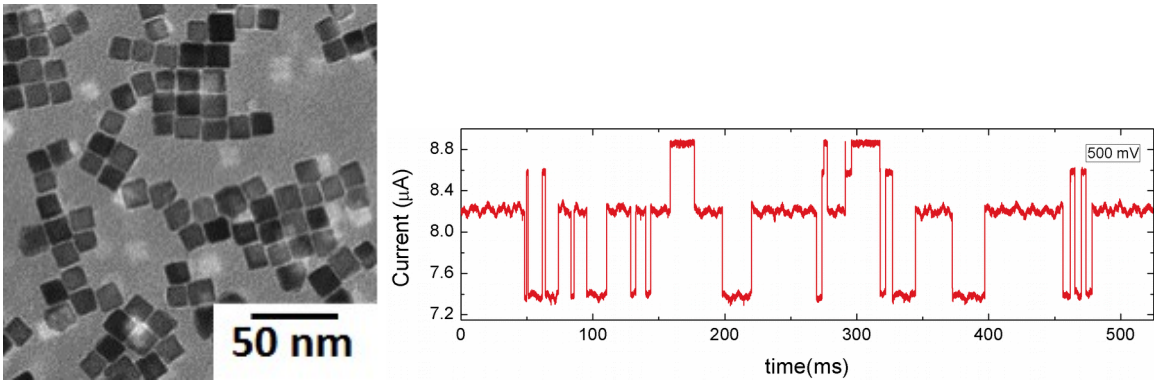

Fig. 3. TEM image of iron oxide nanocubes (left) and telegraph noise seen in the tunnel current through a single cube placed on top of a perpendicularly magnetized FePt thin film.

III. Correlation of Antiphase Boundaries and Magnetic Behavior in Fe_3O_4 Nanoparticles

Iron oxide nanoparticles (NPs) are the most commonly used magnetic particles in ferrofluids [Raj 1995] and biomedical applications [Pankhurst 2009]. The performance of the particles in these applications depends on the magnetic moment, which in turn depends on numerous factors, including the size, shape, and magneto-crystalline anisotropy. High magnetization is desirable, yet most nanoparticles display lower values than the corresponding bulk material. The reduction has been attributed to surface spin disorder [Kodama 1996], [Pratt 2014] or to variations in crystallinity, as in the case of low temperature aqueous preparation methods [Massart 1981]. However, increasing crystallinity and reducing surface roughness does not necessarily solve this problem. The magnetization need not be reduced in small particles.

Our experiments compared 12-14 nm diameter iron oxide nanoparticles synthesized by three well-established methods that were pioneered by the groups of Sun [Sun 2004], Colvin [Yu 2004] and Hyeon [Park 2004]. All three syntheses involve high temperature inert atmosphere decomposition in organic solvents, leading to monodisperse, highly crystalline, spherical particles coated with surfactants. Conventional transmission electron microscopy (TEM) imaging, selected area electron diffraction (SAED), and electron elemental loss spectrometry (EELS) suggested that the particles were quite similar, with no obvious core-shell structure, but their magnetic properties are strikingly different. At 10 K, the Sun particles have a specific saturation magnetization of 81 ± 12 emu/g, values that are roughly 10% below that of the bulk. In comparison, the values for the Colvin particles were 37 ± 1 emu/g, and for the Hyeon particles 39 ± 4 emu/g. These Colvin and Hyeon particles have approximately half the magnetization of the Sun particles of comparable size. A

combination of improved electron microscopy techniques with aberration correction, together with atomistic simulations of the spin configuration, makes it possible to understand the cause of the reduced magnetization.

Depending on the preparation method, even small NPs can support extended structural defects i.e. antiphase boundaries (APBs). While APB defects are seen in almost all substrate supported thin film growth of magnetite these defects are not expected to form in NPs where no film/substrate strain or epitaxial effects (e.g. substrate-film symmetry mismatch) are present [Margulies 1997], [Erenstein 2002], [Gilks 2013]. There is a strong correlation between the reduced magnetization of the magnetite nanoparticles and the presence of APBs. Moreover atomistic magnetic modeling of particles with APBs shows that they have reduced magnetization, and can support multiple magnetic domains even in NPs below 15 nm. While the detection of APBs requires sophisticated atomic resolution electron microscopy, we also saw that zero field cooled magnetization measurements offer a more convenient method of quickly identifying samples with a high density of these defects, and therefore lower magnetization providing the NPs are single crystal phase.

Figure 4 shows atomically-resolved high angle annular dark field (HAADF) images of representative Sun, Colvin and Hyeon NPs. In all three cases the bulk like magnetite structural ordering extends all the way to the particle surfaces without any core-shell like structure. While Sun nanoparticles, such as that shown in Figure 5a, are predominantly spherical with no strain or disorder, antiphase domain boundaries are common in the Colvin and Hyeon particles of Figure 5b-c. The magnetic properties of magnetite are determined by the short-range Fe-O-Fe super-exchange interactions. The dominant super-exchange interaction in Fe_3O_4 between tetrahedral Fe_A and octahedral Fe_B sublattices results in their antiferromagnetic alignment [De Grave 1993], [Mazo-Zuluaga 2007]. The superexchange interactions depend strongly on the angle and the length of the Fe-O-Fe bonds [Goodenough 1955]. When the angle is 90° (the case of Fe_B-O-Fe_B bonds) the super-exchange interaction is ferromagnetic. As the bond angle increases the superexchange becomes antiferromagnetic (AFM), as in the case of 125° Fe_A-O-Fe_B bond that is the dominant superexchange interaction in magnetite. Any further increase in angle, increases the strength of AFM interaction, which reaches a maximum value for 180 ° bonds [Goodenough 1963]. Across the APB the Fe-O-Fe bond angles are distorted which significantly impacts the magnetic properties.

Atomistic spin calculations on model particles (with and without APBs) provided insight into the effect of APBs on the NP magnetization. Using VAMPIRE software [Evans 2014] we calculated the spin configurations at magnetic saturation for various model NPs and compared the results to same size NP without APBs. The calculations for this model NP show that there is a reduction in the saturation magnetization by 20% compared to the same size NP without the structural defect. Furthermore, looking at the spin configuration snapshots one can see the formation of two magnetic domains due to the presence of the strong 180 ° antiferromagnetic bonds across the boundary. Within a domain, the Fe_A and Fe_B spins are antiparallel. Across the APB, the Fe_B spins are canted because of the change in Fe_B-O-Fe_B superexchange coupling. On the other side of the APB the magnetization axis is tilted, so that there is a separate domain.

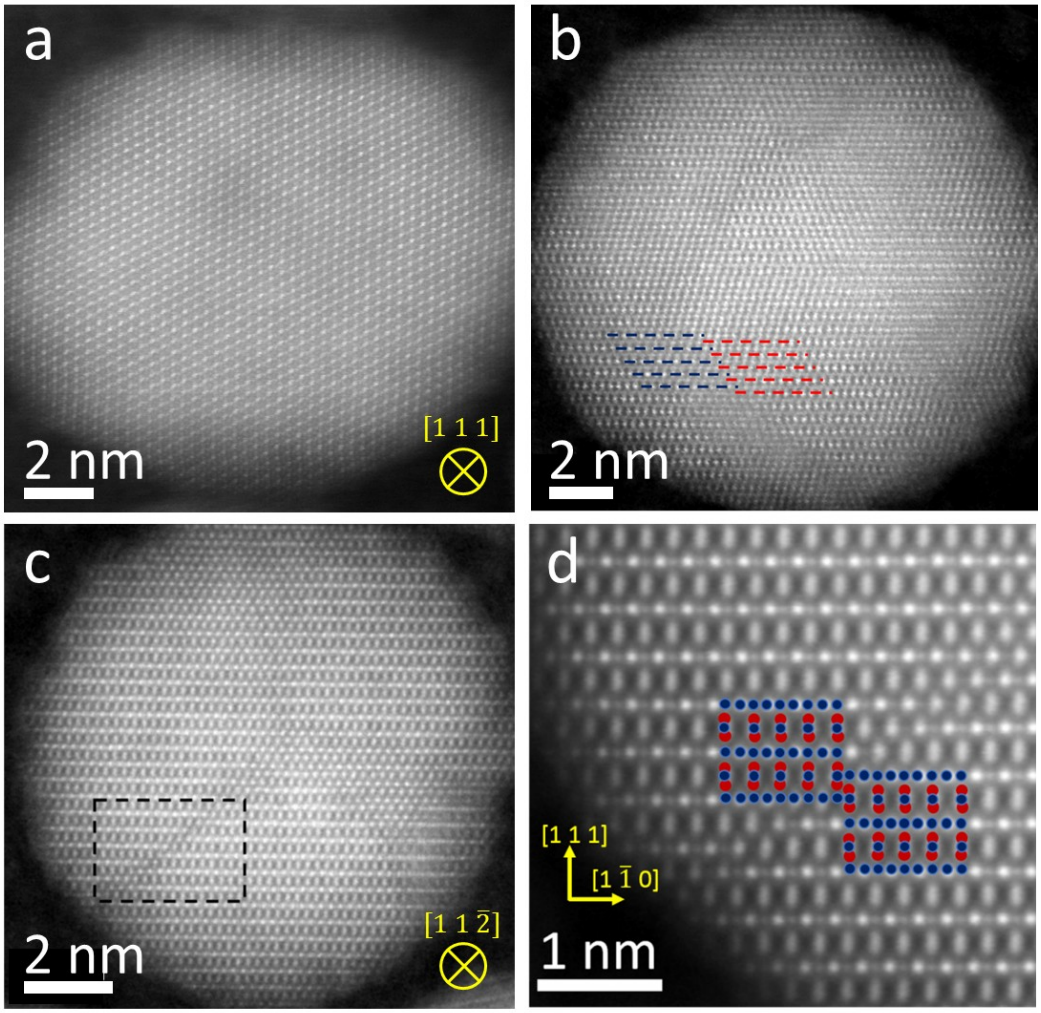

Fig. 4. Atomically resolved HAADF STEM images of representative a) Sun NP viewed along the [111] zone axis, b) Colvin NP viewed along the [114] zone axis. c) Hyeon NP along the [11-2] zone axis, obtained by rigid registration of a stack of images of the same area recorded in quick succession (resulting in high signal-to-noise and precision in the image). Dashed lines in (b) and (c) indicate the presence of the APBs. d) Magnified view of the dashed area shown in (c): an APB with ¼a_0<110> viewed along the [11-2] zone axis.

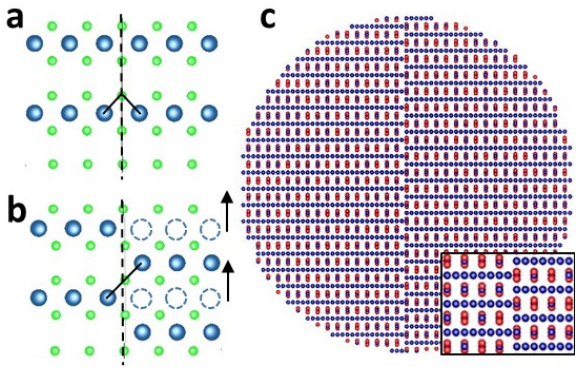

Fig. 5. a) [001] view of a (001) Fe_B–O lattice plane in bulk magnetite. b) The presence of a ¼a_0<110> APB (dashed line) leads to shifted right hand side for ¼a_0<110> (in-plane, arrows represent the shift vector), changing the Fe_B-O-Fe_B angle from 90° as shown in (a) to 180°. The oxygen sub-lattice is invariant under the shift. c) 10 nm nanoparticle model with single ¼a_0<110> APB shown along the [11-2] zone axis. Tetrahedral Fe_A atoms are coloured in red, octahedral Fe_B in blue and oxygen atoms (not shown in (c)) in green.

IV. Polarized Small Angle Neutron Scattering and Spin Configurations in Ferrite Nanoparticles

With polarized SANS, the incident beam of neutrons is polarized "Up" or "Down" by a supermirror, and after passing through the sample, the scattered neutrons are analyzed by passing through a ^{3}He detector that has been pumped with a diode laser and rf source so that is acts as an analyzer for Up (U) or Down (D) neutrons [Chen 2004]. Four cross-sections are measured, two without a neutron spin flip (U to U, D to D) and two weaker spin-flip cross-sections U to D, D to U).

Figure 6 shows an example of the different scattering patterns. Neutrons that do not scatter pass through the central spot in these images. The scattering vector Q between the central beam and the arcs of scattered intensity is indicative of the length scale of order within the sample. For example, the bright arcs in the top images correspond to the (111) spacing of the nanoparticles in the FCC-ordered assembly. The angle θ dependence within the plane of these images enables independent determination of nuclear (structural) scattering and magnetic scattering parallel and perpendicular to an applied magnetic field (here 1.2 T, pointing to the right) [Moon 1969], [Krycka 2012]. While weak, the spin flip scattering is purely magnetic, and so the symmetry of the scattered spin flip intensity conveys subtle information about the spin configuration within the particles. Unlike structural scattering, magnetic scattering depends on the temperature and magnetic field.

Based on both the Q-dependence and the angular dependence of the intensity, a core-shell model of spins within the iron oxide nanoparticle was developed [Krycka 2010], as shown in Figure 7. Without a field the spins are oriented along one of the crystallographic easy axes (E. A.). Within each unit cell, the spins of Fe ions in tetrahedral (A) and octahedral (B) sites point in opposite directions, but there are twice as many B sites, and therefore net ferrimagnetism. With an applied field, there is greater competition between exchange and

Zeeman energies. Spins near the surface have fewer nearest neighbors, and therefore weaker exchange. The relative angle of the tetrahedral and octahedral spins begins to tilt, and a shell is created. Relative spin canting in a magnetic field has been observed by Mössbauer spectroscopy for other types of ferrite nanoparticles [De Grave 1993]. This was assumed to be a surface effect, but without the length scale information provided by neutron scattering it was previously impossible to detect an ordered shell or to determine the average canting angle. A simplified energetic model was created to understand the relative importance of exchange, Zeeman, anisotropy and dipolar energies, in order to be able to predict the conditions for shell formation [Krycka 2014]. It works qualitatively, and successfully predicted the lack of shell formation in 11 nm $CoFe_2O_4$ nanoparticles, which have much higher magnetocrystalline anisotropy [Hasz 2014].

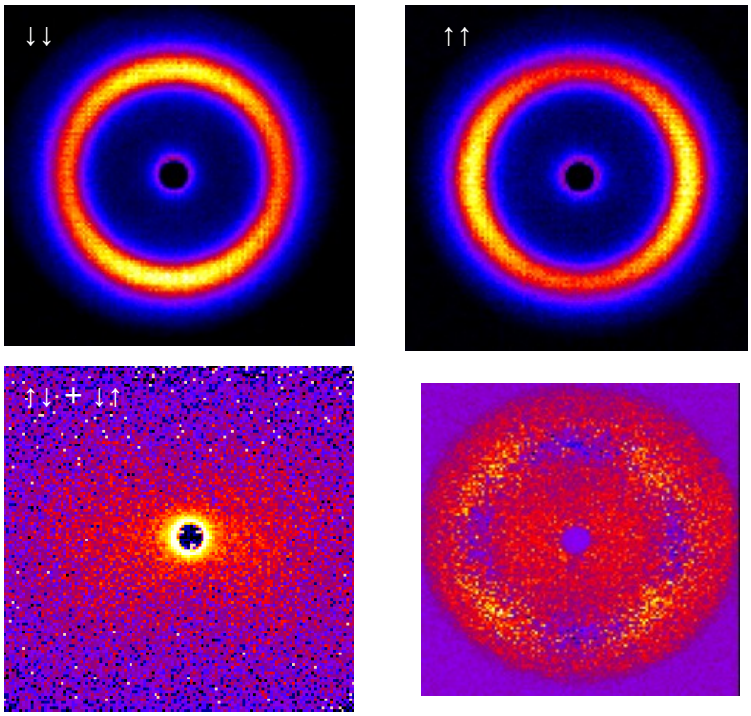

Fig. 6. Two-dimensional detector showing the intensity I(Q, θ) of scattered neutrons for 9 nm Fe_3O_4 nanoparticle assemblies with D to D (upper left), U to U (upper right), the sum of U to D and D to U (lower left) and the difference of U to D and "D to U (lower right).

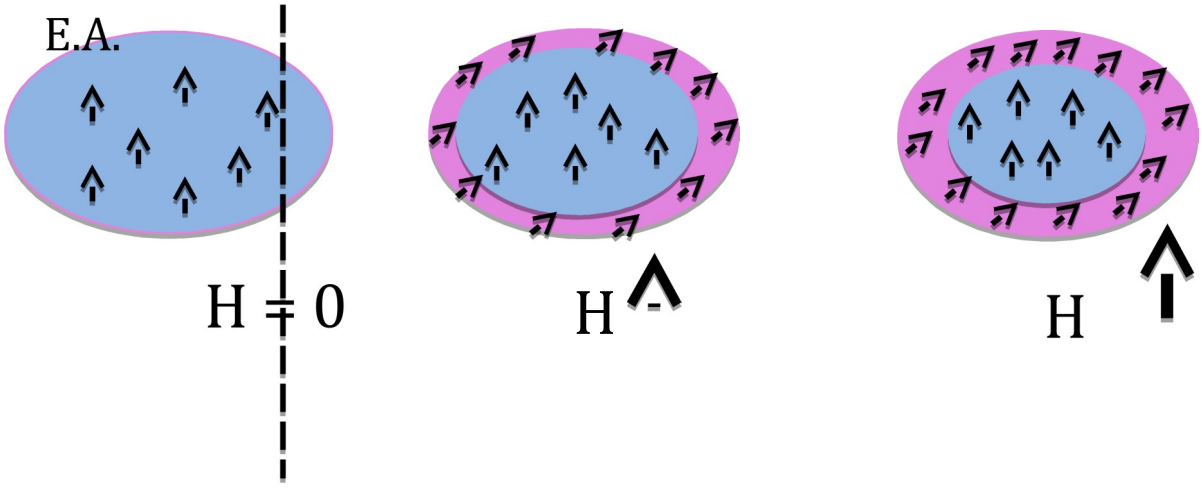

Fig. 7. Schematic of the reversible shell formation of 9 nm Fe_3O_4 nanoparticles in an applied magnetic field. For simplicity, only the net spin per formula unit is shown.

While the reversible core-shell results have received a lot of attention [Krycka 2015a], they have also been controversial [Michels 2015], [Krycka 2015b]. Work continues with the comparison of different magnetic oxide nanoparticles (Mn and Co ferrite) which have different exchange and anisotropy energies, respectively, relative to those of Fe_3O_4. This research is also now coupled with efforts in aberration corrected TEM, where preliminary results show evidence of surface reconstruction. If so this could modify the exchange energy near the surface so that the spins are more susceptible to canting in an external field. Work is also ongoing with the VAMPIRE atomistic simulations of nanoparticles using first principles calculations of exchange and anisotropy for the surface. The goal is to understand the origin of the magnetically driven core-shell formation.

REFERENCES

[Booth 2012] R. A. Booth and S. A. Majetich, "The Magnetocaloric Effect in Thermally Cycled Polycrystalline Ni-Mn-Ga", J. Appl. Phys. **111**, 07A933 (2012).

[Chen 2004] W. C. Chen, T. R. Gentile, K. V. O'Donovan, J. A. Borchers, and C. F. Majkrzak, Polarized neutron reflectometry of a patterned magnetic film with a ^{3}He analyzer and a position-sensitive detector, Rev. Sci. Instrum. **75**, 3256-3263 (2004).

[Chowdary 2013] K. M. Chowdary, Ph. D. thesis, Physics Department, Carnegie Mellon University.

[Chowdary 2014] K. M. Chowdary and S. A. Majetich, "Frequency-Dependent Magnetic Permeability of $Fe_{10}Co_{90}$ Nanocomposites", J. Phys. D: Appl. Phys. **47**, 175001 (2014).

[De Grave 1993] E. De Grave, R. M. Persoons, R. E. Vandenberghe, and P. M. A. de Bakker, "Mössbauer study of the high-temperature phase of Co-substituted magnetites, $Co_xFe_{3-x}O_4$. I. x≤0.04.",Phys. Rev. B, **47**, 5881-5893 (1993).

[Erenstein 2002] W. Eerenstein, T. T. M. Palstra, T. Hibma, and S. Celotto, "Origin of the increased resistivity in epitaxial Fe_3O_4 films. Phys. Rev. B, **66**, 201101(R) (2002).

[Evans 2014] R. F. L. Evans, W. J. Fan, P. Chureemart, T. A. Ostler, M. O. A. Ellis, and R. W. Chantrell, "Atomistic spin model simulations of magnetic nanomaterials", Journal of Physics: Cond. Matt., **26**, 103202 (2014).

[Gilks 2013] D. Gilks, L. Lari, J. Naughton, O. Cespedes, C. Cai, A. Gerber, S. M. Thompson, K. Ziemer, and V. K. Lazarov, "Origin of anomalous magnetite properties in crystallographic matched heterostructures: $Fe_3O_4(111)/MgAl_2O_4(111)$", J. Physics: Condensed Matter **25**, 485004 (2013).

[Goodenough 1955] J. B. Goodenough, and A.L. Loeb, "Theory of Ionic Ordering, Crystal Distortion, and Magnetic Exchange Due to Covalent Forces in Spinels". Phys. Rev. **98**, 391-408 (1955).

[Goodenough 1963] Goodenough, J. B., *Magnetism and the chemical bond*. Vol. 98. 1963: Interscience publishers New York.

[Hasz 2014] K. Hasz, Y. Ijiri, K. L. Krycka and J. A. Borchers, R. A. Booth, S. D. Oberdick, and S. A. Majetich, "Particle Moment Canting in $CoFe_2O_4$ Nanoparticles", Phys. Rev. B **90**, 180405(R) (2014).

[Kodama 1996] R. H. Kodama, A. E. Berkowitz, C. J. McNiff, Jr., and S. Foner, "Surface Spin Disorder in $NiFe_2O_4$ Nanoparticles", Phys. Rev. Lett.. **77**, 394-397 (1996).

[Krycka 2010] K. L. Krycka, J. A. Borchers, J. A. Borchers, Y. Ijiri, W. C. Chen. S. M. Watson, M. Laver, T. R. Gentile, S. Harris, L. R. Dedon, J. J. Rhyne, and S. A. Majetich, "Visualizing Core-Shell Magnetic Interplay within Iron Oxide Nanoparticles", Phys. Rev. Lett. **104** 207203 (2010).

[Krycka 2012] K. Krycka, J. Borchers, Y. Ijiri, R. Booth, and S. Majetich, "Polarization-analyzed small-angle neutron scattering. II. Mathematical angular analysis", J. Applied Crystallography **45**, 554-565 (2012).

[Krycka 2015b] K. L. Krycka, J. A. Borchers, R. A. Booth, S. A. Majetich, Y. Ijiri, and J. J. Rhyne, "Krycka et al. Reply". Phys. Rev. Lett. **114**, 149702 (2015).

[Krycka 2015a] K. L. Krycka, J. A. Borchers, R. A. Booth, S. A. Majetich, Y. Ijiri, and J. J. Rhyne, "Origin of Surface Canting within Fe_3O_4 Nanoparticles", Phys. Rev. Lett. **113**, 147203 (2014).

[Margulies 1997] D. T. Margulies, F. T. Parker, M. L. Rudee, F. E. Spada, J. N. Chapman, P. R.

Aitchison, and A. E. Berkowitz, "Origin of the Anomalous Magnetic Behavior in Single Crystal Fe_3O_4 Films", Phys. Rev. Lett. **79**, 5162-5165 (1997).

[Massart 1981] R. Massart, " Preparation of aqueous magnetic liquids in alkaline and acidic media", IEEE Trans. Mag. **17**, 1247-1248 (1981).

[Mazo-Zuluaga, 2007] J. Mazo-Zuluaga, J. Restrepo, and J. Mejía-López, "Surface anisotropy of a Fe_3O_4 nanoparticle: A simulation approach", Physica B: Cond. Matt., **398**, 187-190 (2007).

[Michels 2015] A. Michels, D. Honecker, S. Erokhin, and D. Berkov, "Comment on 'Origin of Surface Canting within Fe_3O_4 Nanoparticles'", Phys. Rev. Lett. **114**, 147901 (2015).

[Moon 1969] R. M. Moon, T. Riste, and W. C. Koehler, "Polarization Analysis of Thermal Neutron Scattering", Phys. Rev. **181** 920 (1969).

[Nedelkowski 2016] Z. Nedelkoski, D. Kepaptsoglou, L. Lari, T. Wen, R. A. Booth, S. D. Oberdick, D. Gilks, Q. M. Ramasse, R. F. L. Evans, S. A. Majetich and V. K. Lazarov, "Origin of reduced magnetization and domain formation in small magnetite nanoparticles," (Nature Communications, under review).

[Pankhurst 2009] Q. A. Pankhurst, et al., "Progress in applications of magnetic nanoparticles in biomedicine", J. Appl. Phys. D: Applied Physics, **42**, 224001 (2009).

[Park 2004] J. Park, K. An, Y. Hwang, J.-G. Park, H.-J. Noh, J.-Y. Kim, J.-H. Park, N. –M. Hwang, and T. Hyeon, "Ultra-large –scale syntheses of monodisperse nanocrystals", Nat. Mater. **3**, 891 – 895 (2004).

[Piotrowski 2014] S. K. Piotrowski, M. F. Matty, and S. A. Majetich, "Magnetic Fluctuations in Individual Superparamagnetic Particles", IEEE Trans. Mag. **50**, 2303704 (2014).

[Pratt 2014] A. Pratt, L. Lari, O. Hovorka, A. Shah, C. Woffinden, S. P. Tar, C. Binns, R. Kröger., "Enhanced oxidation of nanoparticles through strain-mediated ionic transport", Nat. Mater., **13**, 6-30 (2014).

[Raj 1995] K. Raj, B. Moskowitz, and R. Casciari, "Advances in ferrofluid technology", J. Magn. Magn. Mater. **149**, 174-180 (1995).

[Sakharov 2014] V. K. Sakharov, R. A. Booth, and S. A. Majetich, "High-frequency permeability of Ni and Co particle assemblies", J. Appl. Phys. **115**, 17A517 (2014).

[Stamps 2014] R. L. Stamps, S. Breitkreutz, J. Åkerman, A. V. Chumak, Y. Otani, G. E. W. Bauer, J.-U. Thiele, M. Bowen, S.A. Majetich, M. Kläui, I. L. Prejbeanu, B. Dieny, N. M. Dempsey, and B. Hillebrands, "The 2014 Magnetics Roadmap", J. Phys. D: Appl. Phys.**47**, 333001 (2014).

[Sun 2004] S. Sun, H. Zeng, D. B. Robinson, S. Raoux, P. M. Rice, S. X. Wang, and G. Li,

"Monodisperse MFe_2O_4 (M = Fe, Co, Mn) Nanoparticles", J. Amer. Chem. Soc., **126**, 273-279 (2004).

[Yu 2004] W. W. Yu, J. C. Faulkner, C. T. Yavuz, and V. L. Colvin., "Synthesis of monodisperse iron oxide nanocrystals by thermal decomposition of iron carboxylate salts", Chem. Comm., 2306-2307 (2004).